Emergent Materials (2022) 5:315–321
https://doi.org/10.1007/s42247-022-00352-4

ORIGINAL ARTICLE

Evaluation of bacterial cellulose/quince seed mucilage composite scaffold for wound dressing

Deniz Oran[1] · **Semra Unal**[2,3] · **Oguzhan Gunduz**[3,4]

Received: 8 December 2021 / Accepted: 19 January 2022 / Published online: 3 February 2022

Abstract
Bacterial cellulose (BC) and quince seed mucilage are very promising biological materials. In this study, we reported the design and fabrication of a novel biocompatible scaffold with excellent fibroblast cell proliferation, making it a promising composite scaffold for wound dressings. The composite scaffold was fabricated by ex situ modification of bacterial cellulose by quince seed mucilage. The products were investigated to determine their morphological features, chemical features, and thermal and swelling behaviors. Cell culture and proliferation tests were performed to obtain information on biocompatibility of the scaffolds. This work indicates the novel scaffold provides great potential in wound dressing for clinical application.

Keywords Bacterial cellulose · Quince seed mucilage · Skin tissue engineering · Scaffold · Cellulose dressing

1 Introduction

A wound can be defined as the disruption or damage to the pre-existing anatomical function or structure. Thus, the physiological changes in the organism to repair the wound is the process of "wound healing." Wound healing is a fundamental yet complex physio-biological process classically involving four stages: (1) hemostasis and coagulation; (2) inflammation; (3) proliferation; and (4) remodeling. An ideal wound dressing should have some properties to improve the healing process by protecting the wound from infection, keeping a moist wound circumference to enhance epithelial regrowth, and absorbing exudates around the wound [1, 2].

Quince is the only member in the Rosaceae family belonging to the genus *Cydonia*. Quince harvest of the fruit-bearing and deciduous tree, *Cydonia oblonga*, it has a golden-yellow outer skin and is grown in about every region and climate, mostly in Asia, South Africa, Central Europe, and in the Middle East with Turkey as the primary producer.

A prominent remedy utilized particularly by Eastern medicine since time immemorial, quince has been observed to have anti-inflammatory [3], antioxidant [4], and wound healing [5] properties over time. Further research on quince fruit has likewise proved a positive effect on various diseases such as ulcerative colitis [4] and colon cancer [6]. Different parts of the quince fruit have been observed to have a positive effect on various free radical–related detriments on organisms and diseases such as quince leaf [7], seeds [5], pulp, and peel [8].

The mucilage obtained via the quince seed-water solution is a carbohydrate-based biopolymer. As a polysaccharide which can be quickly dissolved in water, it consists of a superporous, biocompatible, super-absorbent hydrogel that is economical and readily available [9]. The results of various studies indicate that the quince seed mucilage has also been observed to stimulate a wound healing effect on organisms [5, 10, 11].

Cellulose is a readily available polysaccharide and the essential component to the cell wall of green plants. Carboxymethyl cellulose, a chemical modification of cellulose, is one of the most important polysaccharides widely used in the manufacture of wound dressings due to its cost-effectiveness and high demand worldwide [12]. Certain genera of bacteria such as *Acetobacter xylinum* (= *Gluconacetobacter xylinus*) are equally capable of realizing cellulose

✉ Oguzhan Gunduz
ucemogu@ucl.ac.uk

1 Department of Life Sciences, Faculty of Sciences, University of Montpellier, Montpellier, France

2 Institute of Neurological Sciences, Marmara University, Istanbul, Turkey

3 Center for Nanotechnology & Biomaterials Application and Research, Marmara University, 34722 Istanbul, Turkey

4 Department of Metallurgy and Materials Engineering, Faculty of Technology, Marmara University, Istanbul, Turkey

production, with *Gluconacetobacter xylinus* being the most efficient and preferred bacterium [13]. Bacterial cellulose, through its differing properties from plant-originated cellulose, shows a high degree of polymerization, high mechanical strength, high crystallinity, high water-holding capacity, biocompatibility, and moldability [14–16]. The unique properties of this material show promising results in its medical use for wound healing [2, 17–19]. The results of various studies indicate that topical applications of BC membranes improve the healing process of burns and chronic wounds. Different materials have also been integrated with bacterial cellulose in order to improve the healing process of burns and chronic wounds [2, 17, 18, 20–22].

The present study investigates the wound healing capacity of the bacterial cellulose-quince seed mucilage (BC-QSM) scaffold through a series of qualitative, quantitative, and in vitro analyses with the objective to provide a medically used, cost-effective, and biocompatible wound dressing material.

2 Materials and methods

2.1 Preparation of bacterial cellulose/quince seed mucilage composite scaffold

Hestrin-Schramm (HS) medium for *Gluconacetobacter xylinus* ATCC 70,078 consisted of 2.0 wt% D-glucose, 0.5 wt% peptone, 0.5 wt% yeast extract, 0.27 wt% disodium hydrogen phosphate, and 0.115 wt% citric acid, and the pH was adjusted to 5.0–6.0 with acetic acid and the BC pellicles were prepared as previously reported by our group (Fig. 1(a),(b)) [23].

Quince seed mucilage (QSM) was extracted using the hot water extraction method as reported in our previous study [9, 24]. Briefly, seeds (100 g) were soaked in deionized (DI) water for 6 h and heated to 50 °C for 30 min (Fig. 1(c)). Separation of extruded mucilage was accomplished using a cotton cloth. The extruded mucilage was washed with n-hexane and DI water to get defatted and purified mucilage. Further, QSM was collected as sediment after centrifuging the mucilage. The isolated QSM was then heated in an oven at 60 °C to form a dry film. The yield of QSM was calculated as approximately 9% based on weight dried seeds.

The wet BC pellicle was placed between two sheets of filter paper to remove free water. Then, it was immersed in a QSM-dissolved distilled water for 24 h in room condition (Fig. 1(c)). After that, it was withdrawn from the vessel, and the excess QSM solution was removed using filter paper. Finally, it was dried in the oven at 40 °C for 20 h (Fig. 1(e)).

2.2 Characterization of BC and BC/QSM scaffolds

The structure of the BC and BC/QSM composites with different ratios was investigated by FT-IR analysis (VERTEX 70, Bruker, Germany). The spectra were collected over the range from 400 to 4000 cm^{-1}. The surface morphology and the structure of BC, QSM, and BC/QSM scaffolds were characterized by scanning electron microscopy (SEM, EVO MA-10, ZEISS Inc., USA) with an accelerating potential of

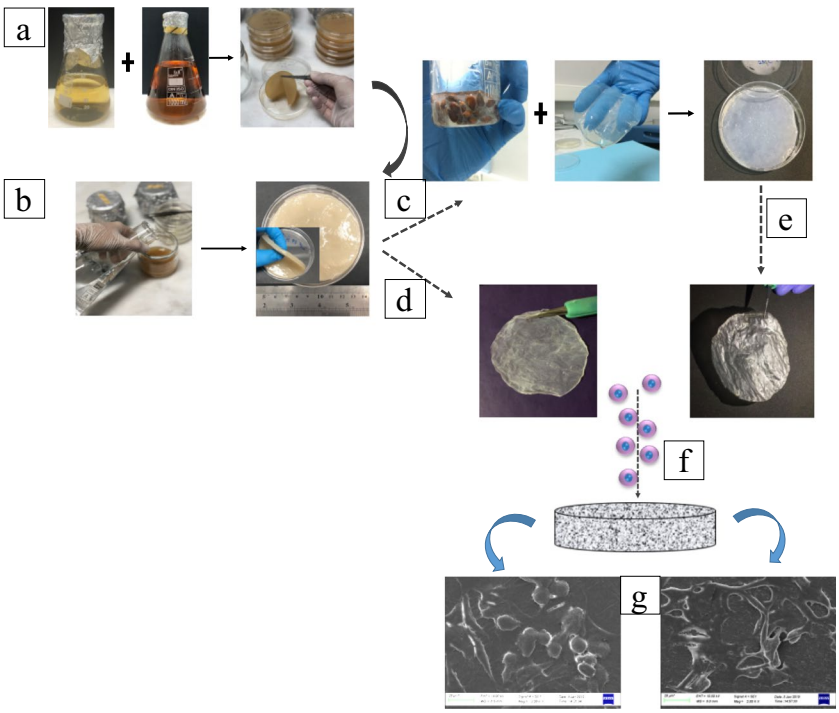

Fig. 1 Schematic illustration of fabrication of bacterial cellulose (BC) pellicle and quince seed mucilage (QSM) scaffolds. **a** The static phase was performed at 28 °C for 14 days and then produced BC. **b** BC pellicles were soaked into 0.1 M NaOH solution at 100 °C for 2 h for alkali treatment, then washed with deionized water, and then they were autoclaved at 120 °C for 20 min. **c** BC pellicle was immersed in QSM for 24 h at ambient temperature. **d** Oven-dried BC scaffold. **e** Oven-dried BC/QSM composite scaffold. **f** Fibroblasts were cultured on the BC and BC/QSM scaffolds. **g** Cell morphology observed using a scanning electron microscope

10.0 kV and magnifications of 1000–5000. The oven-dried samples were sputter-coated with gold for 60 s.

2.3 Swelling analysis

The swelling ratios of BC and BC/QSM composite scaffolds were determined as reported previously [14]. Briefly, a weighed dry scaffold was soaked in PBS (pH 7.4, 37 °C) during predetermined time intervals (up to 12 h) at ambient temperature. The bandage samples were taken out from the medium and excess fluid remaining on the surface was gently removed by filter paper and reweighed. The swelling ratio was evaluated using the following formula:

$$\text{Swelling ratio} = \frac{Ws - Wd}{Wd} \text{x} 100$$

where W_d is the dry and W_s is the post swelling weight of each scaffold after a particular time.

2.4 Differential scanning calorimetry (DSC) thermal analysis

BC, QSM, and BC/QSM samples were weighed as 5.7 mg and placed separately into aluminum pans and closed. A small pinhole was punched on the top of the aluminum pan. DSC analysis of the samples was performed by using nitrogen gas with the Hitachi 7000X DSC instrument. Three consecutive runs (heating–cooling-heating) were conducted in the range of − 80 °C to 260° C with a heating rate of 10 °C/min.

2.5 In vitro biocompatibility and cell morphology analysis

The BC and BC/QSM scaffolds were cut into 16-mm disks and placed into 24-well plates, and then the prepared samples were sterilized using UV radiation for 2 h and incubated with Dulbecco's modified Eagle's medium (DMEM) for 24 h before cell seeding. Fibroblasts were cultured on the BC, BC/QSM, and tissue culture polystyrene (TCP) at a cell density of 2.5×10^4 cells/well with DMEM supplemented with penicillin (100 units per mL), streptomycin (100 µg Ml^{-1}), and 10% fetal bovine serum in a humidified atmosphere of 5% CO_2 and 95% air at 37 °C (Fig. 1(f)). After 48 h, BC and BC/QSM scaffolds were transferred to a new culture well to eliminate the possibility of false positive by cells that may have attached on the well. Spent medium was replaced with 100 µL fresh medium of complete DMEM. Ten microliters (10 µL) of MTT was added into every well and cells were incubated at 37 °C for 4 h. One hundred microliters (100 µL) of DMSO solution was then added, and after another 4 h of incubation, the solution was transferred to a 96-well plate and absorbance was read at 570 nm using a spectrophotometer reader.

At day 2, cell-laden scaffolds were fixed with 2.5% glutaraldehyde (Sigma) and then dehydrated through serial dilutions of ethanol and dried in air. Dried specimens were sputter-coated with gold and observed using a scanning electron microscope (SEM) (EVO MA-10, Zeiss, Germany) with an accelerating voltage of 10 kV (Fig. 1(g)).

3 Results and discussion

3.1 Fabrication and structural analysis of BC and BC/QSM scaffolds

QSM was successfully isolated using the hot water extraction method, and the percentage yield was estimated to be 9 g/100 g of seeds.

The surface morphology of the pure BC, pure QSM, and BC/QSM composite scaffold as examined by SEM is shown in Fig. 2. Figure 2A presents the SEM images of dried QSM. As shown in Fig. 2B, a well-organized three-dimensional fibrillary network was observed for pure BC scaffold. On the other hand, BC/QSM composite scaffold was even more compact probably due to the presence of QSM on the surface (Fig. 2C). It was clearly shown that QSM might penetrate the pores of bacterial cellulose and interact with the microfibrils of BC, which may affect the physicochemical properties. While the ribbons and pore structure of the native cellulose presented clearly, BC/QSM composite scaffold formed a denser network structure and decreased the pore size.

3.2 Structural characterization, swelling, and differential scanning calorimetry of the scaffolds

The presence of QSM in the bacterial cellulose scaffold was proved by FT-IR analysis. For this purpose, FT-IR spectra of QSM, BC, and BC/QSM were recorded and compared with FT-IR spectra of a powder blend of these excipients as depicted in Fig. 3. In FT-IR spectrum of QSM, the presence of characteristic peaks 1730, 1620, and 1420 cm^{-1} reflected the presence of carbonyl group (C = O) indicating the presence of uronic acid residues in QSM that contains a large fraction of hemicelluloses [9, 25, 26]. The band observed at 1730 cm^{-1} is attributed to the carbonyl stretching of –COOH. Furthermore, the characteristic band at 1620 cm^{-1} is due to C = O asymmetric stretching in carboxylate anion that is reconfirmed by another sharp peak at 1420 cm^{-1} which is related to the symmetric stretching mode of the carboxylate anion [25]. The presence of glycosidic linkage (C–O–C) vibrations in polysaccharide is reflected by the peaks

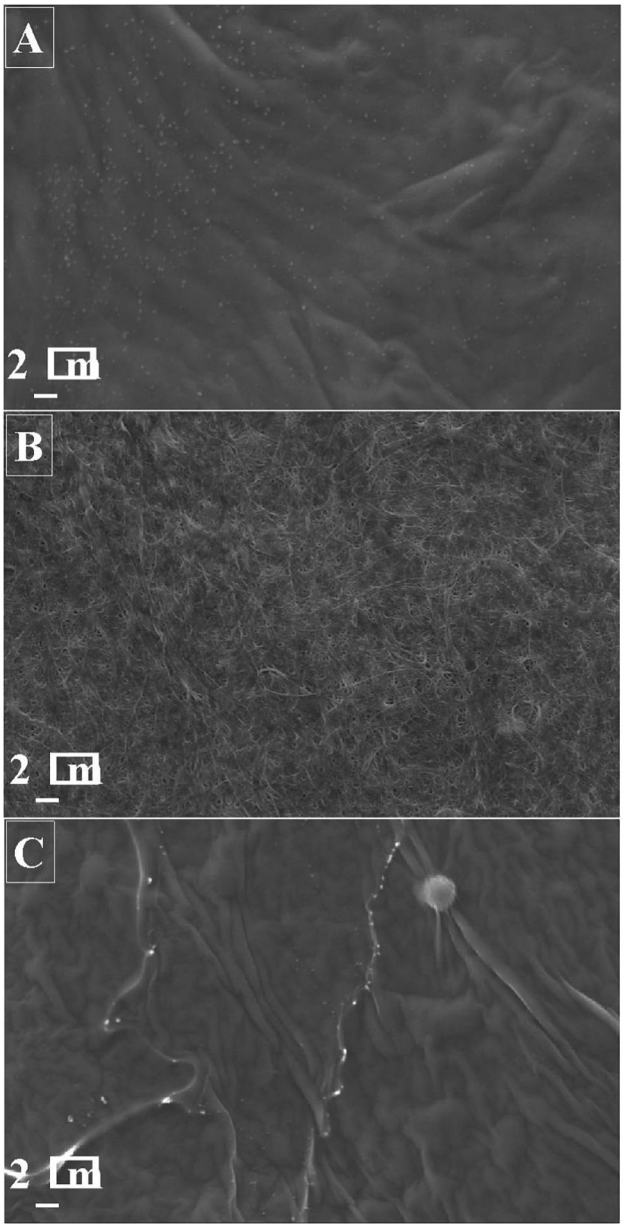

Fig. 2 SEM images of (**A**) QSM, (**B**) BC, and (**C**) BC/QSM scaffolds

appearing at between 1000 and 1200 cm^{-1} [9, 26]. The broad band performed at 3800–2700 cm^{-1} is the characteristic stretching peaks of O–H (3600–3100 cm^{-1}) and C-H (2950–2800 cm^{-1}) [9, 25, 26]. For the pure BC, a broad characteristic band at 3300 cm^{-1} is attributed to O–H stretching vibration. The band at 2940 and 2820 cm^{-1} presents the aliphatic C–H stretching vibration [27]. The absorbance peak at wave number 1730 cm^{-1} is attributed to the hydrogen-bonded carbonyl stretching vibration [27]. Another sharp band observed at 1080 cm^{-1} was ascribed to the presence of C–O–C stretching vibrations [18, 27]. The above-mentioned characteristic bands of BC

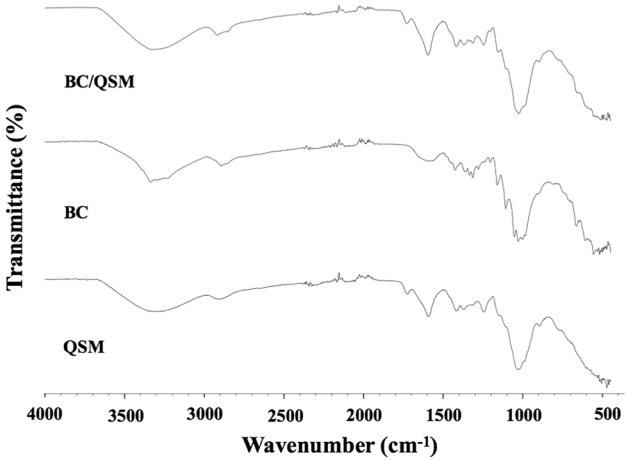

Fig. 3 FT-IR spectra of QSM, BC, and BC/QSM scaffolds

and QSM were present in combination with the BC/QSM scaffold, thus confirming that QSM was embedded in the BC structure.

3.3 Swelling study

The capacity to maintain a moisture-absorbing environment is a crucial factor for wound dressing materials, and according to previous studies, BC addition increases the water absorbance and wicking ability. In this study, the percent swelling results for BC and BC/QSM composite scaffolds for various water contact times are depicted in Fig. 4.

The scaffold composed of QSM showed the highest swelling ratio that reached 3681 ± 17% after 6 h while pure BC reached the highest swelling capacity 790 ± 8% after 1 h. The ex situ QSM-modified scaffolds exhibited the highest swelling ratio: 2318 ± 11% after 0.5-h immersion in PBS,

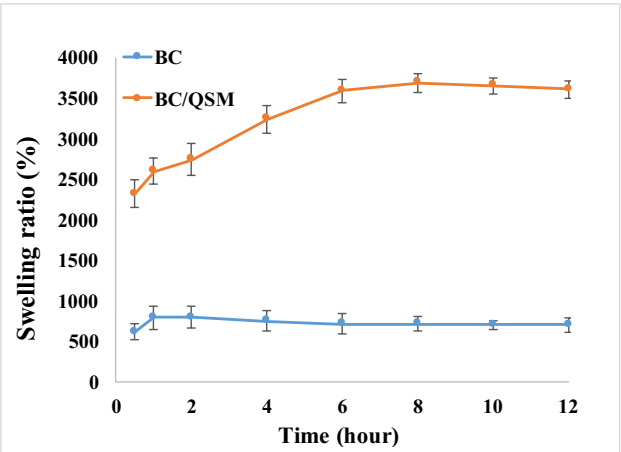

Fig. 4 Swelling behavior of BC and BC/QSM scaffolds

reached full capacity at 3681 ± 17% after 6 h, and stabilized 3605 ± 14% after 12 h. These values in each time interval are much higher than those observed for the pure bacterial cellulose scaffolds, showing the influence of the hydrophilicity of QSM on the liquid swelling capacity of the scaffolds. The presence of QSM in the BC/QSM scaffolds resulted in the increase in liquid uptake capacity. In case of phosphate buffers of pH 7.4, rapid swelling is attributed to the deprotonated form of a carboxyl group present in the polysaccharide (QSM) resulting in electrostatic repulsive forces within polymer chains, and consequently, extensive swelling was observed [9]. Due to their high water content, BC/QSM composite materials are appealing as a scaffold because they resemble natural soft tissue, which includes the skin.

3.4 Differential scanning calorimetry

Differential scanning calorimetry (DSC) studies of BC-based scaffold incorporated with QSM were performed to further understand the structure and interaction between BC and QSM. Melting temperature (Tm) and glass transition temperature (Tg) can be associated with the crystallinity of the samples [11]. Data of DSC analysis for three different samples are reported in Table 1. Examining the values in Table 1, the melting point of BC was found to be 63.4 °C. While the glass transition temperature of QSM was − 53.8 °C and the melting point was 170.7 °C. For the BC/QSM composite, on the other hand, the glass transition temperature of QSM in the composite slightly increased to − 53.1 °C, whereas the melting point decreased to 152.1 °C. However, the addition of QSM increased the melting point of BC to 75.3 °C in the composite; this could be attributed to the larger molecular weight and more hydrophilic nature of QSM (Fig. 5).

As a consequence of these findings, incorporation of QSM to the composite system had an enhancing effect on thermal properties [11]. On the other hand, the thermal properties of QSM decreased with the addition of BC to the composite; a similar effect was reported in the literature [28]. Moreover, the BC incorporation to the BC/QSM composite reduced the working range of the material and the thermal properties.

Despite the enhanced biological properties, obtained by incorporating BC to the composite, the reduced thermal properties are compensated by the addition of QSM to the system.

Table 1 DSC data of the BC, QSM, and BC/QSM scaffolds

Sample name	Tg (°C)	$Tm_{(QSM)}$ (°C)	$Tm_{(BC)}$ (°C)
BC	-	-	63.4
QSM	− 53.8	170.7	-
BC/QSM	− 53.1	152.1	75.3

Tg glass transition temperature, *Tm* melting temperature

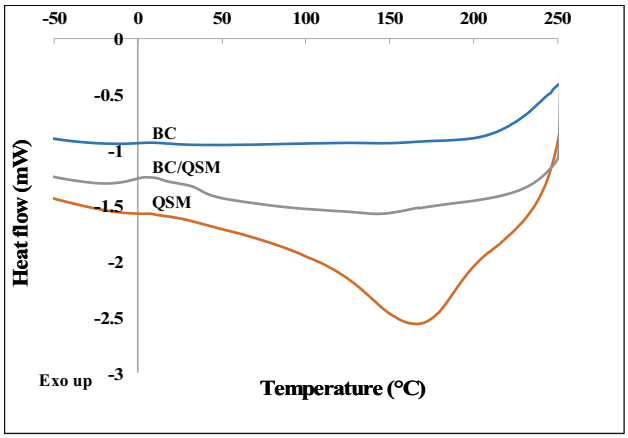

Fig. 5 DSC thermograms of the QSM, BC, and BC/QSM scaffolds

3.5 Cytotoxicity and cell attachment

Wound healing is a complex, dynamic process supported by blood cells, extracellular matrix, and parenchymal cells [10]. Fibroblasts are the main cell type that promotes neoangiogenesis in the regulation of ECM protein production for the proper development of blood vessels, secretes all extracellular matrix (ECM) components, and produces a variety of cytokines and growth factors [5]. The in vitro biological properties of BC and BC/QSM were analyzed by measuring the cytotoxicity and cell attachment. The previous studies reported excellent biocompatibility of BC scaffold for animal fibroblast and osteoblast cells [17, 29]. Similarly, several studies indicated the ability of QSM to stimulate the proliferation of human skin fibroblast [5, 10]. The superiority of three-dimension (3D) cell culture has been demonstrated compared with TCP (two-dimension, 2D) cell cultures. Fibroblast cells have demonstrated accelerated proliferation and better extracellular matrix synthesis on 3D scaffolds compared with that on conventional 2D cell culture [29]. Our results revealed that BC and BC/QSM scaffolds significantly enhanced the proliferation rate of fibroblast cells after 48 h of treatment compared to the 2D cell culture; on the other hand, fibroblast cells proliferated slower on the BC/QSM scaffolds compared to BC controls (Fig. 6). This preliminary experiment suggests that QSM can accelerate wound healing [10]. On the other hand, the proliferation of fibroblast cells was reduced in BC/QSM scaffolds (Fig. 6) compared to BC controls due to 3D environmental factors such as limited nutrient and oxygen diffusion because of the reduced porous structure.

Figure 7 shows the cell attachment on pure BC and BC/QSM composite. Fibroblast cells were seeded on cylinder

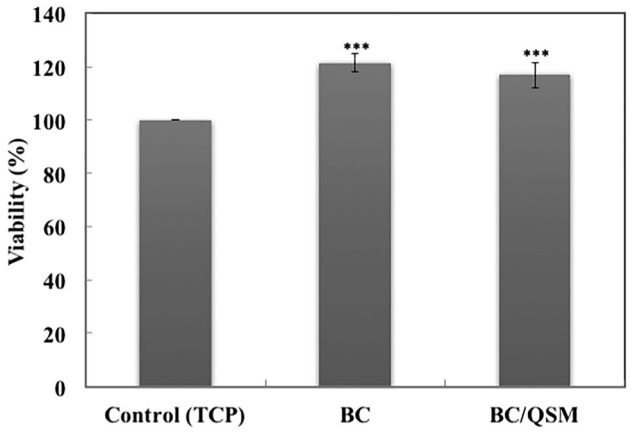

Fig. 6 Percentage of fibroblast cell viability on the control (TCP), BC, and BC/QSM. All statistical analysis was performed by using GraphPad Prism (GraphPad Software, San Diego, CA). Data were considered statistically significant for a p value < 0.001

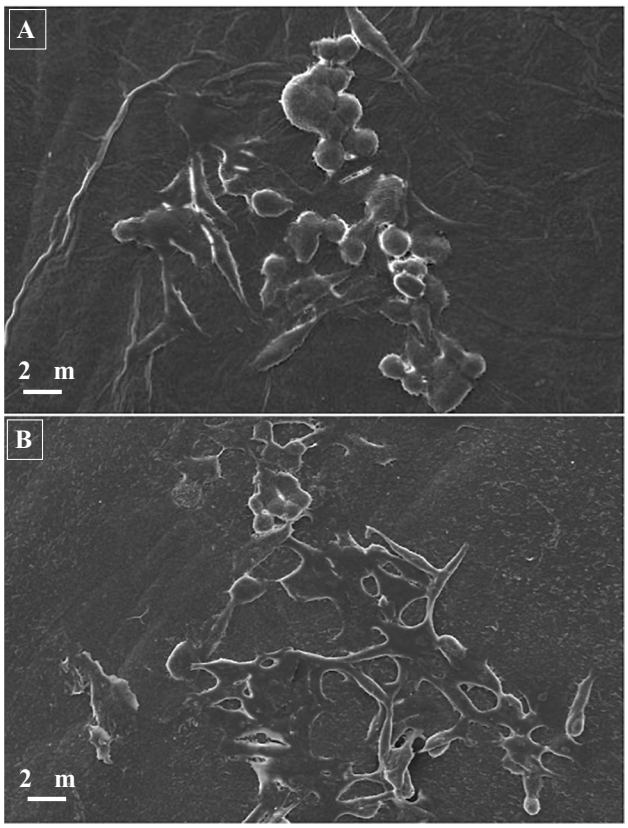

Fig. 7 Fibroblast cell adhesion on the (**A**) BC and (**B**) BC/QSM scaffolds on day 2: SEM images of cell-material interactions. The scale bar is 2 µm

scaffolds. After 48 h of incubation, there were many cells attached on pure BC scaffolds (Fig. 7(A)). Most of the cells remained in round shape, which means the cells do not tend to proliferate. For BC/QSM scaffolds, cells adhered and completely spread on the surface (Fig. 7(B)). They had many pseudopodia and formed a layer on the surface. These results indicated that the cells stretched their morphology and were increasing. The reason may be due to the incorporation of QSM. As introduced before, QSM can enhance cell adhesion and proliferation. QSM can create a natural extracellular environment that is important for cell communication and layer formation. It would have potentials to be used as wound dressing materials.

4 Conclusion

BC and BC/QSM scaffolds were successfully prepared in this study. SEM images showed that pore structure of BC changed morphologically with the addition of quince seed mucilage. The presence of QSM in BC led to a more compact fibrillary network with a closed pore structure. Results from the increased swelling behavior of BC/QSM composite scaffold indicate that it could provide a suitable moisture environment for wound healing applications. We reported that enhancement of fibroblast proliferation and attachment by BC/QSM supports medical use of this natural composite scaffold for wound dressing.

Funding This work was supported and funded by Marmara University Scientific Researches Committee (BAPKO) (FEN-C-DRP-110718–0402).

Declarations

Conflict of interest The authors declare no competing interests.

References

1. E.Y.X. Loh, N. Mohamad, M.B. Fauzi, M.H. Ng, S.F. Ng, M.C.I. Mohd Amin, Development of a bacterial cellulose-based hydrogel cell carrier containing keratinocytes and fibroblasts for full-thickness wound healing. Sci. Rep. **8**, 1–12 (2018). https://doi.org/10.1038/s41598-018-21174-7
2. S. Ye, L. Jiang, J. Wu, C. Su, C. Huang, X. Liu, W. Shao, Flexible amoxicillin-grafted bacterial cellulose sponges for wound dressing: in vitro and in vivo evaluation. ACS Appl. Mater. Interfaces. **10**, 5862–5870 (2018). https://doi.org/10.1021/acsami.7b16680
3. M. Minaiyan, A. Ghannadi, M. Etemad, P. Mahzouni, A study of the effects of Cydonia oblonga Miller (quince) on TNBS-induced ulcerative colitis in rats. Res. Pharm. Sci. **7**, 103–110 (2012). https://pdfs.semanticscholar.org/f714/50052bb74c71d57283d45d81dcc0c92044d2.pdf?_ga=2.168406690.202106262.1549234561-900931602.1546849390 (Accessed Feb 4, 2019)
4. M. Jouki, S.A. Mortazavi, F.T. Yazdi, A. Koocheki, Optimization of extraction, antioxidant activity and functional properties of quince seed mucilage by RSM. Int. J. Biol. Macromol. **66**, 113–124 (2014). https://doi.org/10.1016/j.ijbiomac.2014.02.026
5. P. Tamri, A. Hemmati, M. Ghafourian, Wound healing properties of quince seed mucilage : in vivo evaluation in rabbit

full-thickness wound model. Int. J. Surg. **12**, 843–847 (2014). https://doi.org/10.1016/j.ijsu.2014.06.016
6. M.M. Ahmed, G.A. Elmenoufy, 6- Quince polysaccharides induced apoptosis in human colon cancer cells (HCT-116). Res. Cancer Tumor **5**, 1–9 (2016). https://doi.org/10.5923/j.rct.20160501.01
7. R.M. Costa, A.S. Magalhães, J.A. Pereira, P.B. Andrade, P. Valentão, M. Carvalho, B.M. Silva, Evaluation of free radical-scavenging and antihemolytic activities of quince (Cydonia oblonga) leaf: a comparative study with green tea (Camellia sinensis). Food Chem. Toxicol. **47**, 860–865 (2009). https://doi.org/10.1016/J.FCT.2009.01.019
8. A.S. Magalhães, B.M. Silva, J.A. Pereira, P.B. Andrade, P. Valentão, M. Carvalho, Protective effect of quince (Cydonia oblonga Miller) fruit against oxidative hemolysis of human erythrocytes. Food Chem. Toxicol. **47**, 1372–1377 (2009). https://doi.org/10.1016/J.FCT.2009.03.017
9. M.U. Ashraf, M.A. Hussain, S. Bashir, M.T. Haseeb, Z. Hussain, Quince seed hydrogel (glucuronoxylan): evaluation of stimuli responsive sustained release oral drug delivery system and biomedical properties. J. Drug. Deliv. Sci. Technol. **45**, 455–465 (2018). https://doi.org/10.1016/j.jddst.2018.04.008
10. M. Ghafourian, P. Tamri, A. Hemmati, Enhancement of human skin fibroblasts proliferation as a result of treating with quince seed mucilage, Jundishapur J Nat Pharm. Prod. **10**, 10–13 (2015)
11. M. Jouki, S.A. Mortazavi, F.T. Yazdi, A. Koocheki, Characterization of antioxidant-antibacterial quince seed mucilage films containing thyme essential oil. Carbohydr. Polym. **99**, 537–546 (2014). https://doi.org/10.1016/j.carbpol.2013.08.077
12. V. Kanikireddy, K. Varaprasad, T. Jayaramudu, C. Karthikeyan, R. Sadiku, Carboxymethyl cellulose-based materials for infection control and wound healing: a review. Int. J. Biol. Macromol. **164**, 963–975 (2020). https://doi.org/10.1016/j.ijbiomac.2020.07.160
13. H. El-Saied, A.H. Basta, R.H. Gobran, Research progress in friendly environmental technology for the production of cellulose products (Bacterial cellulose and its application). Polym. – Plast. Technol. Eng. **43**, 797–820 (2004). https://doi.org/10.1081/PPT-120038065
14. S. Khan, M. Ul-Islam, M. Ikram, M.W. Ullah, M. Israr, F. Subhan, Y. Kim, J.H. Jang, S. Yoon, J.K. Park, Three-dimensionally microporous and highly biocompatible bacterial cellulose-gelatin composite scaffolds for tissue engineering applications. RSC Adv. **6**, 110840–110849 (2016). https://doi.org/10.1039/C6RA18847H
15. M. Ul-Islam, T. Khan, J.K. Park, Water holding and release properties of bacterial cellulose obtained by in situ and ex situ modification. Carbohydr. Polym. **88**, 596–603 (2012). https://doi.org/10.1016/j.carbpol.2012.01.006
16. A. Azarniya, N. Eslahi, N. Mahmoudi, A. Simchi, Effect of graphene oxide nanosheets on the physico-mechanical properties of chitosan/bacterial cellulose nanofibrous composites. Compos Part A Appl. Sci. Manuf. **85**, 113–122 (2016). https://doi.org/10.1016/j.compositesa.2016.03.011
17. Z. Cai, J. Kim, Preparation and characterization of novel bacterial cellulose/gelatin scaffold for tissue regeneration using bacterial cellulose hydrogel. J. Nanotechnol. Eng. Med. **1**, 021002 (2010). https://doi.org/10.1115/1.4000858
18. W.C. Lin, C.C. Lien, H.J. Yeh, C.M. Yu, S.H. Hsu, Bacterial cellulose and bacterial cellulose-chitosan membranes for wound dressing applications. Carbohydr. Polym. **94**, 603–611 (2013). https://doi.org/10.1016/j.carbpol.2013.01.076
19. M. Moniri, A. BoroumandMoghaddam, S. Azizi, R. Abdul Rahim, A. Bin Ariff, W. ZuhainisSaad, M. Navaderi, R. Mohamad, Production and status of bacterial cellulose in biomedical engineering. Nanomaterials **7**, 257 (2017)
20. S. Khan, M. Ul-Islam, W.A. Khattak, M.W. Ullah, J.K. Park, Bacterial cellulose-titanium dioxide nanocomposites: nanostructural characteristics, antibacterial mechanism, and biocompatibility. Cellulose **22**, 565–579 (2015). https://doi.org/10.1007/s10570-014-0528-4
21. J. Kim, Z. Cai, H.S. Lee, G.S. Choi, D.H. Lee, C. Jo, Preparation and characterization of a bacterial cellulose/chitosan composite for potential biomedical application. J. Polym. Res. **18**, 739–744 (2011). https://doi.org/10.1007/s10965-010-9470-9
22. B. Fang, Y. Wan, T. Tang, C. Gao, K. Dai, Proliferation and osteoblastic differentiation of human bone marrow stromal cells on hydroxyapatite/Bacterial. Tissue Eng. Part A **15**, 1091–1099 (2009)
23. E. Altun, M.O. Aydogdu, M. Crabbe-Mann, J. Ahmed, F. Brako, B. Karademir, B. Aksu, M. Sennaroglu, M.S. Eroglu, G. Ren, O. Gunduz, M. Edirisinghe, Co-culture of keratinocyte- *Staphylococcus aureus* on Cu-Ag-Zn/CuO and Cu-Ag-W nanoparticle loaded bacterial cellulose:PMMA bandages. Macromol. Mater. Eng. **304**, 1800537 (2019). https://doi.org/10.1002/mame.201800537
24. M.U. Ashraf, M.A. Hussain, G. Muhammad, M.T. Haseeb, S. Bashir, S.Z. Hussain, I. Hussain, A superporous and superabsorbent glucuronoxylan hydrogel from quince (Cydonia oblanga): stimuli responsive swelling, on-off switching and drug release. Int. J. Biol. Macromol. **95**, 138–144 (2017). https://doi.org/10.1016/j.ijbiomac.2016.11.057
25. H. Hosseinzadeh, S. Mohammadi, Quince seed mucilage magnetic nanocomposites as novel bioadsorbents for efficient removal of cationic dyes from aqueous solutions. Carbohydr. Polym. **134**, 213–221 (2015). https://doi.org/10.1016/j.carbpol.2015.08.008
26. C. Ritzoulis, E. Marini, A. Aslanidou, N. Georgiadis, P.D. Karayannakidis, C. Koukiotis, A. Filotheou, S. Lousinian, E. Tzimpilis, Hydrocolloids from quince seed: extraction, characterization, and study of their emulsifying/stabilizing capacity. Food Hydrocoll. **42**, 178–186 (2014). https://doi.org/10.1016/j.foodhyd.2014.03.031
27 T.D. Lopes, I.C. Riegel-Vidotti, A. Grein, C.A. Tischer, P.C. de Sousa Faria-Tischer, Bacterial cellulose and hyaluronic acid hybrid membranes: production and characterization. Int. J. Biol. Macromol. **67**, 401–408 (2014). https://doi.org/10.1016/j.ijbiomac.2014.03.047
28. H.S. Barud, C.A. Ribeiro, M.S. Crespi, M.A.U. Martines, J. Dexpert-Ghys, R.F.C. Marques, Y. Messaddeq, S.J.L. Ribeiro, Thermal characterization of bacterial cellulose – phosphate composite membranes. **87** 815–818 (2007)
29. S. Khan, M. Ul-Islam, M. Ikram, S.U. Islam, M.W. Ullah, M. Israr, J.H. Jang, S. Yoon, J.K. Park, Preparation and structural characterization of surface modified microporous bacterial cellulose scaffolds: a potential material for skin regeneration applications in vitro and in vivo. Int. J. Biol. Macromol. **117**, 1200–1210 (2018). https://doi.org/10.1016/j.ijbiomac.2018.06.044